

Article citation info:

Mączak J, Więclawski K, Szczurowski K, New approach of model based detection of early stages of fuel injector failures. *Eksploracja i Niezawodność – Maintenance and Reliability* 2023; 25(1) <http://doi.org/10.17531/ein.2023.1.6>

## New approach of model based detection of early stages of fuel injector failures

Indexed by:



Jędrzej Mączak<sup>a</sup>, Krzysztof Więclawski<sup>a\*</sup>, Krzysztof Szczurowski<sup>a</sup>

<sup>a</sup> Warsaw University of Technology, Faculty of Faculty of Automotive and Construction Machinery Engineering, Narbutta 84, Warsaw, Poland

### Highlights

- Electric waveforms controlling fuel injectors were presented along with their mathematical modelling.
- Typical injector failures and the ways of detecting them using electric current signals were described.
- Model-based method for early detection of failures in electromagnetic valves was proposed.

### Abstract

The aim of the work was to develop a method of real time diagnosing electromagnetic fuel injectors using the observation of electric current parameters available in the engine control unit. Performing this task required finding a precise criterion for assessing the correct operation of an electromagnetic injector. For this purpose, a mathematical model describing the individual phases of the injector's operation was used, allowing the simulation of the occurrence of typical failures. On its basis, symptoms of particular failures were determined based on the observation of electric current parameters in the control circuit. Observation of voltage and current waveforms allows to locate both electrical and mechanical damages to the injectors and to assess the correctness of the power system components. The presented diagnostic method allows the detection of the described damages in the early stages of their development, which prevents damage to the catalytic converter and other engine systems (valves, piston rings or cylinder surfaces), i.e. damages resulting from an incorrect fuel mixture.

### Keywords

electromagnetic fuel injectors, technical diagnostics, failure, fault, symptom, damage, model-based diagnosis

This is an open access article under the CC BY license (<https://creativecommons.org/licenses/by/4.0/>)

### 1. Introduction

Observation of changes in electric characteristics of the valves used allows for detection of changes in their operation at an early stage of damage development and for taking action before they can affect the system's reliability [39, 40]. Observation of residual values, i.e. differences between values derived from the model and from the real measurement [27], enables conclusions regarding not only the injector's technical state but also the type and size of the damage [41].

In the case of a particular type of an electromagnetic valve, which is the fuel injector used in internal combustion engines (ICEs), even operation under the initial fault can lead to mechanical damage in the ICE systems or the system of exhaust gas purification and to the negative influence on the amount of toxic substances in such an engine exhaust gas. Fig. 1 shows a general view of an exemplary gasoline injector used in combustion engines.



Fig. 1. Electromagnetic fuel injector.

Work of a fuel injector in a car ICE is controlled by the diagnostic system – On Board Diagnostics (OBD) and by means of the engine's electronic control unit (ECU). The control system embedded in the control unit performs its diagnostic functions on the injector mainly through measurements of its electric circuit resistance. The OBD can, apart from measurements of the circuit continuity, determine the faulty operation of the injector

(\*) Corresponding author.  
E-mail addresses:

J. Mączak (ORCID: 0000-0002-5460-5588) [jedrzej.maczak@pw.edu.pl](mailto:jedrzej.maczak@pw.edu.pl), K. Więclawski (ORCID: 0000-0002-3004-7956) [krzysztof.wieclawski@pw.edu.pl](mailto:krzysztof.wieclawski@pw.edu.pl), K. Szczurowski (ORCID: 0000-0002-2187-5776) [krzysztof.szczurowski@pw.edu.pl](mailto:krzysztof.szczurowski@pw.edu.pl)

by detecting incorrect dosage (incorrect parameters of exhaust gas as determined by the sensors controlling the mixture). Despite the highly restrictive standards required by the legislator for the content of toxic substances in the exhaust [9, 20], the OBD system can detect only critical injector damage, such as: the discontinuity in the powering circuit or coil, or the total blockage of the needle closing the nozzle. In the course of operation, the injector, as an element susceptible to high load conditions (temperature, pressure, and frequency of work), may be subject to partial damage causing deterioration of its work parameters [5]. Damage such as: changes in the circuit resistance, increase in the connectors resistance, partial jamming of the needle in the channel, partial blockage of the orifices dosing the fuel, short-circuit in the coil winding (bypass) decreasing the generated magnetic flux, change in the characteristic of the return spring, or a slight short-circuit to the minus, are not properly identified by the OBD system [11, 18]. Initial phases of damage may remain unnoticed in the course of the engine work if more detailed bench testing is not performed on the disassembled injector. As a result of the abovementioned types of damage, the engine work takes place with too lean or too rich a mixture [36].

## 2. Problem specification

Diagnostics of fuel injectors is performed in the combustion engines using multiple methods, which could be divided into methods that can be applied during engine operation of the actuator or after its removal from the engine. Stationary methods on the test stand allow for a precise damage assessment, but they are troublesome due to the need to take the vehicle out of service. Due to the digital actuator management the usage of automatic methods of technical state verification of injectors is possible. One of the approaches is diagnostics based on a model determining the correct operation of the actuator.

In the currently applied solutions, the model-based diagnostics could be performed automatically due to the implementation of algorithms used to assess similarities between the model sets of data and measurement data [13, 15, 22]. Model-based diagnostics is hugely popular. The frequency [30] and time [14, 23] domain are typically used for the mathematical description. Mathematical models are used to estimate the combustion processes and to determine composition of combustion gases generated in the cylinder during a single cycle, however the injector diagnostics relying on the observation of its behaviour in the course of the actual work is not an easy task [17, 19]. The model presented in the article [17], consists of two main sub-models for air charge and tail gas. The air charge submodel estimates the mass of trapped air and total residual gas, and the temperature of the gas in the cylinder. The tail gas submodel calculates exhaust backflow during valve overlap by recording the gas exchange dynamics. Exhaust gas retraction into the cylinder is estimated using a compressible ideal gas model for engines equipped with variable valve timing (VVT). The cycle-based model output parameters are in good agreement with dynamic experimental data with minimal lag and overshoot. In an article [19], Leach et al. uses a Coriolis mass flow meter (CFM), which is used to

measure the fuel flow rate through individual fuel injectors in real time, which allows for dose comparisons.

Optical methods allow an accurate assessment of the results of the injection, but they can only be used for bench measurements [28]. Wu et al. [42], presents the analysis of the process of fuel atomization, atomization and evaporation of droplets, thanks to the rapid imaging technique [31]. The impact of control parameters and nozzle geometry on the injection process and thermodynamic changes were examined. Similarly, in the article [43], Yosukawa et al. analyzed the atomization of fuel escaping from the injector nozzle. Due to comparative simulations carried out using the laser Doppler method, the size of droplets formed was determined. Using the photoelectric phenomenon, Bor et al. [3], presented a diagnostic method that allows observation of injection growth, its assessment and determination of injection start and end. Merola et al. [24] presented another optical method., which, using an endoscopic system coupled with a CCD camera, analyzes the structure and rate of change of the state of the expanding fuel after exiting the injector nozzle. In the last cited work, Alloca et al. [1] thanks to the vision method, analyzes the quality of injection with the simultaneous use of a microphone for measuring acoustic emissions, Fourier analysis and wavelet analysis, assessing the phenomenon of atomization of the fuel mixture.

The vibroacoustic methods mentioned above are the most popular methods of diagnostics, and what is important, possible to perform during the engine work of the injector. This diagnostic method is used by Putwattana et al. [29], examining the injector acoustic signal during the simulation of its various damages. It has been proven that damage can be identified based on an acoustic signal with greater efficiency than based on a vibration signal. Injector diagnostics based on acoustic and vibration signals are presented in the article [8]. Figlus et al. presents in it the frequency distribution of vibration signals and noise emitted by the engine and how, after occurrence of damage to the injection system, the frequency structure of the identified vibroacoustic signals changes. In [25] the method of classification for detecting faults in the injectors based on the features extracted from the acoustic signals was presented. Lin et al [21] used in-cylinder pressure and acoustic emission to detect the simulated injector fault in both time and frequency domains.

Vibration signals are the basis for the considerations presented by Nogin et al. [26]. Using time-frequency analysis and low power accelerometers, the occurrence of damage to the engine and its accessories was determined. Similarly, Jiamin et al. [16], searches for damage to the injection system based on the measurement of engine head vibration.

Diagnosis of the injector on the test bench is very accurate, however, it requires removing the injector from the vehicle engine, which is naturally associated with taking it out of service. Hence, methods are sought that allow verification, but without interruptions in the use of the vehicle. Such a method is diagnostics based on control parameters available in the memory of engine controllers – ECU [6]. This approach is presented by Sarwar et al. [32], which recognizes changes in the functioning of the injector by the adaptations stored in the engine controller.

In turn, Gritsenko et al. [10] built a throttle position verification system that corresponds to specific engine responses. Changes in the mapping indicate a malfunction of the fuel injector. The diagnostic parameter here may be the engine speed. Its fluctuations, not related to the change resulting from the control, allow to assess the condition of fuel injectors [37] (Wang et al.). Leach et al [19] presents a different method of injector verification. It is based on the measurement of fuel flow through injectors, carried out through the use of Coriolis flow meters (CFM), characterized by the possibility of measuring as small quantities as individual fuel doses with the possibility of measuring them in real time.

Bozhkov et al [4] and Sebok et al. [34] suggest the possibility of conducting fuel injector verification, based on current waveform analysis. Electric current flowing through the valve coil causes the magnetic flux, and, as a result of its action, the generation of the magnetic force acting on the injector's needle [11]. This force enables lifting the needle (an element cutting off the flow) after all the resisting forces opposing this action have been overcome. Thus, by means of observation of changes in the electric current flowing through the valve coil, the correctness of the opening process can be precisely monitored, i.e. the moment of opening and the value of the electric current [35, 40], at which the opening takes place. Determination of the location in time as well as values in characteristic points for the waveform, and comparison with the theoretical values acquired from the model, allows for determination of the degree of the valve wear and defining the damage in its early stage [33, 41]. Differences in magnitude of parameters, between the modelled time-related voltage and current waveform, relative to the waveforms measured on an ongoing basis, are the residual quantities that may constitute a diagnostic parameter enabling determination not only of the valve's technical condition [12, 39], but also the type and size of the damage. As a result of detection of the change in residual value, indicating an early stage of the valve damage, the valve can be switched off operation or the parameters of its work corrected so as to minimise the wear effect without delay [7, 38] before they can affect the system's reliability [40, 43] This would be a pro-ecological action, with a deep economic impact, since the occurrence of subsequent resultant engine and exhaust purification system damage is prevented.

Considering the above observations and the current state of knowledge, an original diagnostic method was developed. It is a model-based method allowing early detection of failures in electromagnetic valves, comprising vehicle fuel injectors, which would rely on observation of electric signals (current and voltage) in the control system. A set of parameters determining a proper injector operation is assumed as a model utilized for the reference purposes. This is a diagnostic method based on the parameters available while controlling the injector operation that would be possible to be implemented in the vehicle ECU, and applied in real time to modify the injector operation. It is essential that, the electric current parameters observed are a very precise criterion for evaluation of the valve operation. The next chapter presents a fuel injector model based on the Kirchhoff equations, extended by the authors.

### 3. Model of fuel injector operation

The diagnostic procedures described in the subsequent sections of this article are related to the simulated electric current-based waveform generated by the functional mathematical model of the injector with defined control parameters. Fig. 2 illustrates the model waveform (black line) as well as recorded waveforms of the genuine injectors with different faults.

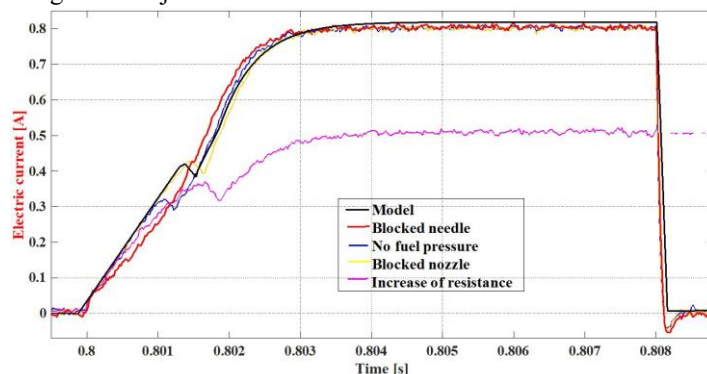


Fig. 2. Electric current-based model waveform (black line) with superimposed experimental waveforms modified by occurrence of different failures.

Electric current-based experimental waveforms shown in Fig. 2 were recorded on a test stand as a result of performing the measurements of the electric current while the injector was working. All of the signals were recorded for the same kind of injector, but with different failures, with similar work parameters. All waveforms presented on Fig. 2 are shown within the same phase offset, due to which they can be compared to each other. The model characteristic reflects the actual controlled dose with injection time  $t = 10$  ms and injection pressure  $p = 0,03$  MPa. Fig. 2 does not include the waveform of the injector with the short circuit because such a fault induces an essential modification in the current waveform, therefore it will be shown individually. The model characteristic of the increasing current waveform was created by the authors on the basis of the Kirchhoff's equation [2], with the determined initial conditions:

$$I_i(t) = f_{press} \frac{\varepsilon_0}{R} \left( 1 - \exp\left(-f_k \frac{R}{L_{1,2}} t\right) \right) - f_p \quad (1)$$

where:  $I$  – electric current, A;  $U_L$  – electric voltage on inductance, V;  $L$  – inductance, H;  $R$  – resistance,  $\Omega$ ;  $\varepsilon_0$  – electromotive force, V;  $t$  – time, s;  $f_{press}$  – coefficient dependant on injection pressure,  $f_p$  – position coefficient,  $f_k$  – directional coefficient. The coefficients are naturally an invariant value for the injector system.

The use of the coefficient  $f_{press}$  in the Kirchhoff's equation is a consequence of the fundamental phenomenon responsible for the shape of the current waveform for the dosing injector, i.e. the overcoming of the forces of resistance ( $F_0$ ) counteracting the lifting of the needle by the magnetic force ( $F_m$ ) in the successive milliseconds of the fuel injection:

$$F_m = f(I, \mu_R, l_S, L) \begin{cases} F_m < F_0 \Rightarrow \frac{dI}{dt} > 0; \\ F_m = F_0 \Rightarrow \frac{dI}{dt} = 0; \\ F_m > F_0 \Rightarrow \frac{dI}{dt} < 0; \\ F_m > F_0 \Rightarrow \frac{dI}{dt} < 0; \end{cases} \quad (2)$$

where:  $\mu_R$  – magnetic permeability of the coil core;  $l_S$  – distance between the needle and centre of the coil core;  $F_m$  – electromagnetic force, N;  $F_0$  – resistance force, N.

#### 4. Real-time model based-diagnostics of the injectors

In model-based diagnostics [23] the mathematical model represents the proper operation of the device and the corresponding simulated quantities are compared to those measured. The emerging differences called residuals are hints about the existence of errors. Typically, the process of calculating the residuals is performed in the frequency domain, as the model describes the injector behavior in time domain the model-based diagnostic process was adopted to the time domain. The concept of this method is shown on Fig. 3.

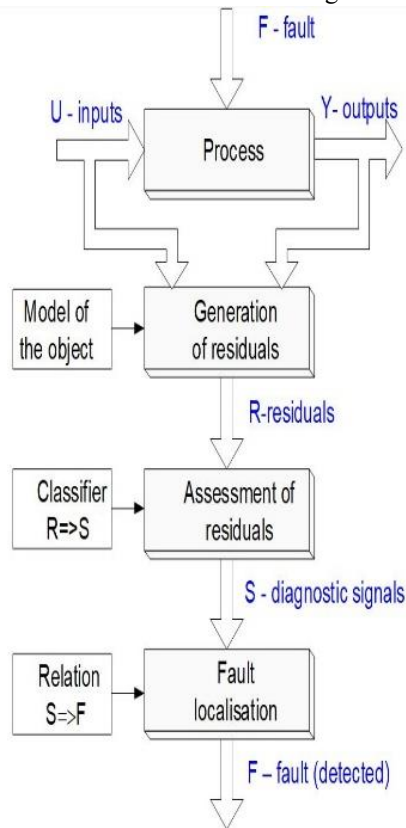


Fig 3. Layout of model-based diagnosis.

In this approach, the term "Process" denotes a system (object) processing certain input quantities ( $U$ ) into output quantities ( $Y$ ) in the presence of faults ( $F$ ). With the adequately identified model of object behaviour, and confronting it with the real input data ( $U$ ), answers of the model can be generated, which comparison with a response of a real system will allow for generation of the residuals, indicating the difference in the real object operation relative to the model. Analysis of the residuals enables creation of classifiers of the object's technical state processing them into diagnostic signals ( $S$ ). These signals allow for determination of the faults of the real object ( $F$ ).

Transforming this to the injector example,  $U$  are the working parameters (injection duration, fuel pressure etc.) and  $Y$  are measured electric current and voltage waveforms measured during the injection. Numerical model generating these waveforms should take into account the set of current working parameters  $U$ .

The proposed, model-based approach in diagnosing early phases of developing faults of dosing valves, relies on comparing the characteristic points of the recorded voltage and electric current waveforms observed during normal work with the values obtained from the model. Differences between these values are residual quantities, which are the measure of the proper (or faulty) operation of the injector.

For the sake of orderly arrangement and clarity of the description, all figures in the subsequent sections of this work, illustrating the fluctuations in characteristics (residuals), have identical denotations/markings, used in accordance with the following equations:

1. Value of the electric current in the steady state (maximum value):

$$I(t) = \frac{\varepsilon_0}{R}. \quad (3)$$

2. Time shift in the phase of the electric current increase – change of any of the components of the exponent index in equation (1):

$$\exp\left(-f_k \frac{R}{L_{1,2}} t\right) \quad (4)$$

3. Change in the electric current at the point of the needle lifting – resulting from the change in any of the parameters on the right of the equation (5) determining the electric current in the steady state:

$$I(t) = f_{press} \frac{\varepsilon_0}{R} \quad (5)$$

4. Phase shift of the point of the needle lifting – resulting from the change in the exponent index (4) and, in consequence, the change in the time constant of the coil  $\tau$ ,

5. Change in the angle of the curve representing the increasing electric current relative to the time axis – changes in equation (4),

6. Change in the voltage value of the inductance peak at its maximum – changes in the electric current, inductance, and changes in the time of the electric current decay:

$$U_L(t) = \frac{dI}{dt} L \quad (6)$$

7. Change in the electric voltage at the point of the needle lowering – modification  $\varepsilon_0$ :

$$U_{L,6}(t) = f_{press} \varepsilon_0 \left( \exp\left(-\frac{R}{L_2(e^{-t})} t\right) \right) + f_p \quad (7)$$

8. Phase shift of the point of the needle lowering – due to the same factors as mentioned above, in Formulae (6) and (7).

In the next sub-chapters several injector faults were analyzed with special focus on their symptoms in the measured electric signals.

#### 4.1 Injector wiring short circuit

This section discusses the changes in electric current-related characteristics, occurring after short circuit of the injector coil. Fig. 4 illustrates the changes of the electric waveforms for three cases of short circuit at different values of resistance (of the flow

value at the point of the short circuit). The left ordinate axis denotes the electrical voltage, the right ordinate axis is the current and photodetector voltage determining the phase of the actual fuel flow. The black line (solid and dotted) marks the model voltage and electric current of the injector. The lines: red, green, and dark blue denote measurements of the current values of the injector coil with the different damages implemented. The analysed damage is a short circuit generated by inserting a 1 Ω, 10 Ω and 20 Ω resistors between the coil supply wires.

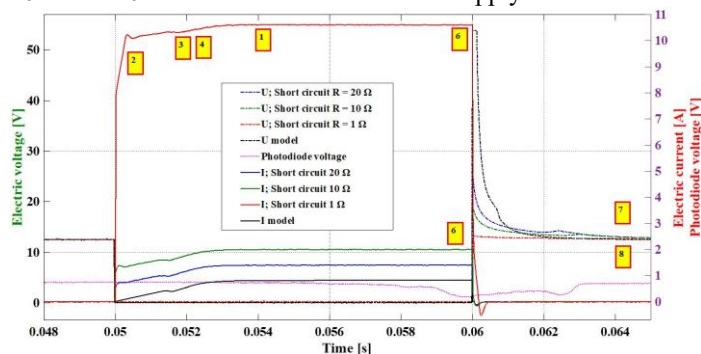


Fig. 4. Overview of residual changes occurring along the short circuit in the injector coil.

In the case of the short circuit with resistance of 1 Ω, 10 Ω, and 20 Ω, the total electric current flowing in the circuit will amount to, respectively:

$R_{Z1} (1 \Omega) \Rightarrow I_{1\Omega} = 12.81 \text{ A}$ ; in the injector coil  $I_1 = 0.81 \text{ A}$ . At the point of the short  $I_z = 12 \text{ A}$ .

$R_{Z10} (10 \Omega) \Rightarrow I_{10\Omega} = 2.01 \text{ A}$ ; in the injector coil  $I_1 = 0.81 \text{ A}$ . At the point of the short  $I_z = 1,2 \text{ A}$ .

$R_{Z20} (20 \Omega) \Rightarrow I_{20\Omega} = 1.41 \text{ A}$ . in the injector coil  $I_1 = 0.81 \text{ A}$ . At the point of the short  $I_z = 0.6 \text{ A}$ .

The electric current in the injector coil does not change. The total electric current changes, of the current flowing through the injector coil and the point where the short occurs. Fig. 4 illustrates all changes (residuals) in the measured electric current waveform after the considered changes have taken place. They were marked with yellow squares on the diagram. They are discussed using the example of one value of the short-circuit (represented by a specific resistor). The residuals have been marked in Fig. 4 by numbers from 1 to 8.

The short circuit results in an increase in the value of the electric current in the steady state (residual #1). The lower the resistance determining the short-circuit, the greater the increase in the electric current in the steady state. Simultaneously, change in the angle between the line of increasing electric current waveform and the abscissa axis is observed (residual #2). The residual #3 denotes an increase in the current at the point of the needle lifting, and the residual #4, a shift in the phase of this point. These changes are very vivid, to a large extent modifying the current-related waveform.

The short circuit is the only damage that introduces the voltage decay in the waveform, after switching off the voltage pulse. These are changes #6, #7 and #8 simultaneously. As mentioned before, the controlled short-circuit does not change the current flow through the injector coil itself. However, the conducted tests have shown the increase of the fuel dose after such a modification. This is a result of the fact that the voltage

decays more slowly, voltage is longer operative in the circuit which ensures that the injector needle is lowered with a visible delay (Fig. 5, fragment from Fig. 4).

For instance, the characteristic marked dark blue, denoting the short-circuit  $R_{Z20} = 20 \Omega$ , identifies the as the point of the needle lowering as  $x = 0.06244 \text{ s}$ , which marks a delay relative to the model characteristic (black dotted line) by 1.76 ms. This means a total delay of flow closure (from switching off the voltage pulse) by  $t_{op} = 2.44 \text{ ms}$ . The photodetector voltage waveform is a proof thereof; these are the changes of the laser beam disturbed by the fuel, determining the real phase of the flow (pink dotted line, bottom of Fig. 5).

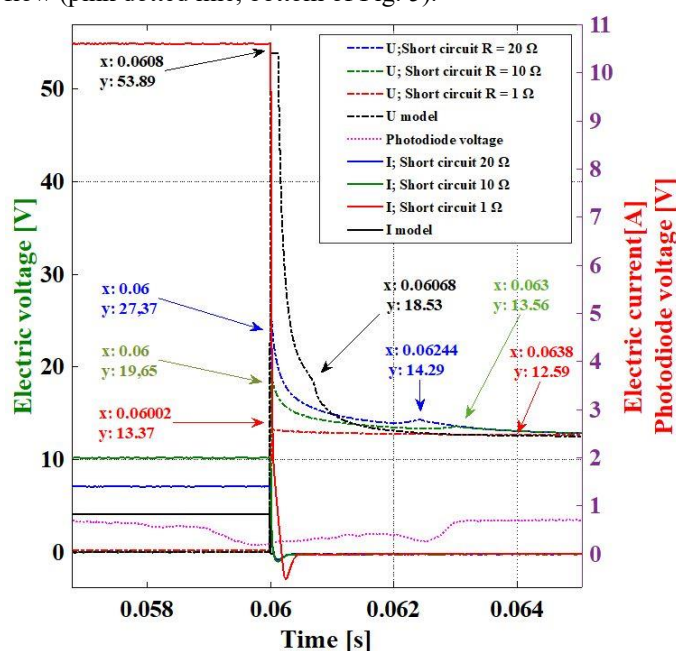


Fig. 5. Fluctuations of values  $U_L$ , phase of the inductance jump and the needle lowering point.

In the case of occurrence of short circuiting reflecting the low resistance values, i.e. crucial short circuit, modifications within the values of the characteristic waveform points as well as the phase fluctuations are very clear and proportional to the value of electric resistance at the point of the short circuit. Especially during the increase phase, the electric current waveform is significantly modified. The controlled short circuit does not affect the needle operation as far as the electric current is concerned, it causes, however, a delay in the needle lowering. As a result, a major shift in phase takes place, and elongation of the real time of the fuel flow.

#### 4.2 Investigation of resistance alteration impact

Fig. 6 shows deviations from the model characteristic, when the resistance  $R$  is increased by 1 Ω, 2 Ω and 10 Ω. In the course of the experiment, this was obtained by inserting series of adequate resistors in the circuit of the injector coil. Increasing the resistance of the coil connector very clearly relates to the modifications within the waveform of the electric current. Resistance of the operational injector coil, in this case amounted to 15 Ω. It can be observed that the change by 10 Ω results in a 40% decrease in the maximal value of the electric current. Residual #2 is the change in the angle between the line of the

increasing electric current waveform and the abscissa axis.

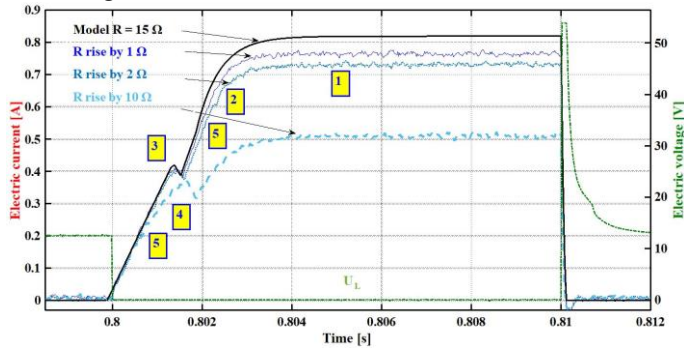


Fig. 6. Differences between the reference (modelled) characteristic and the measurement, in the case of change in the resistance in the injector circuit.

Increasing the connector resistance by 2 Ω (Fig. 6), illustrated in the plot with the blue line, is, most of all, a significant decrease in the maximal values of the electric current in the steady state, described as residual #1. The model in the steady state amounts to  $I(t) = 0.81$  A. A change in resistance from 15 Ω to 17 Ω, renders a result:

$$I(t) = \frac{\varepsilon_0}{R_{17}} = \frac{12.2 \text{ V}}{17 \text{ Ohm}} = 0.717 \text{ A} \quad (8)$$

The subsequent effect of increasing resistance by 2 Ω, is a clear decrease in the slope of the line representing the increasing electric current (residual #5), change in the time constant, i.e. reducing the speed of the current increase. Increasing the connector resistance entails the decrease in the electric current at the needle lifting point (residual #3) and shifting this point in phase (residual #4). The occurrence of such a change results in diminishing the fuel doses and shifting the fuel flow in time.

#### 4.3. Blockage of the injector outlet

Apart from determining the deviations from the model, connected with the change of current-related conditions, it has been verified in the laboratory experiment, what response could be expected in the case of blockage of the injector outlet. Fig. 7 shows an overview and location of the residual quantities, if such a fault should occur.

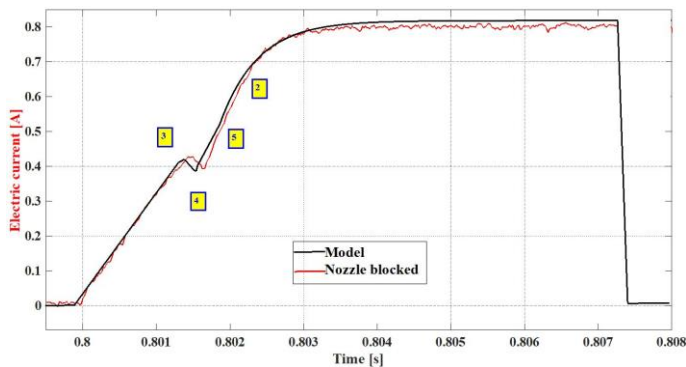


Fig. 7. Residuals #2 to #5 - in the case of blockage of the injector outlet.

As a result of blockage of the injector outlet, the occurrence of residual #2 has been observed by means of measurement, i.e. the shift in phase of the increasing electric current after the needle lifting, and residual #5 – increase in the angle of this line's inclination relative to the time axis. This change takes place due to the shift of the local maximum of the electric current at the point of the needle lifting.

The next change induced by the blockage of the injector outlet is the occurrence of the residual #3 (Fig. 8). This is an increase in the electric current at the point of the needle lifting and a delay in the phase of this point. The fuel does not flow under the needle and does not balance the injection pressure, not even to a lesser degree. In the case when the flow does take place, the fuel gets inside the nozzle and under its upper part, diminishing the difference of pressure values before and after the needle. In the situation, when the flow occurs, the needle is lifted at a lower electric current (i.e. it is able to lift more easily). In the case of the lack of fuel flow, the electric current must reach a greater value to generate a greater magnetic flux and magnetic force (2).

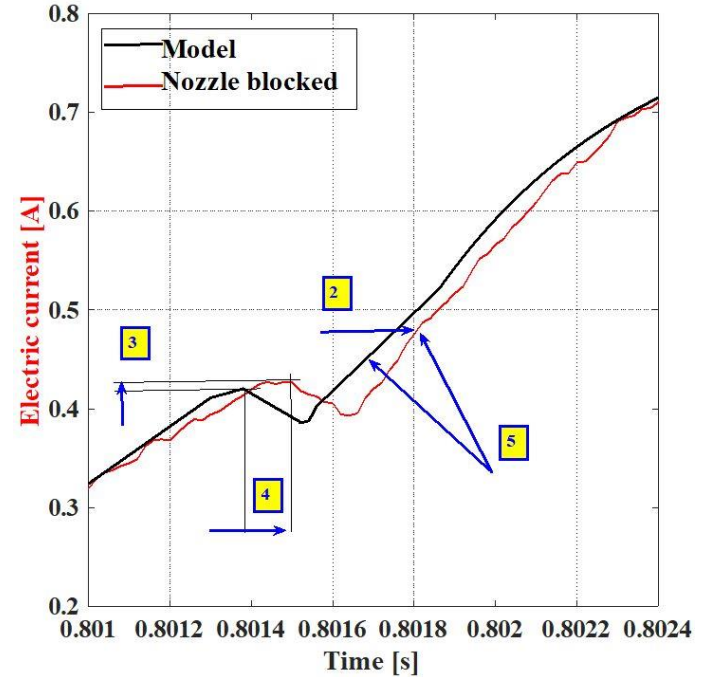


Fig. 8. Residuals #3 and #4 – increase in current  $I_{op}$  and shift into phases of the transient state. Residuals #2 and #5 – shift in the phase of increasing electric current and increase of the angle of the curve relative to time axis.

#### 4.4 Lack of fuel pressure

Fig. 9 illustrates the changes in the electric current-related waveform and their placement, in the situation where there is no injection pressure, relative to the model waveform generated for the value of injection pressure equal to 0.4 MPa. Similarly, to the case of the nozzle blockage, the residuals in this case are not a result of the modifications of the electric current-related parameters. In spite of this, also when there occurs the lack of injection pressure, the emergence of such a fault may be identified, because the changes result from the change in the relation of forces in the equation (2).

The lack of fuel pressure causes fluctuations in the electric current waveform, in the phase of the current increase after the needle lifting. These changes are described as residual #2, connected with the phase shift (negative shift) and residual #5, connected with the increase of the angle of the electric current waveform. Observation of both of them allows for differentiation, whether it is the lack of fuel pressure that has to be dealt with, or the short-circuit, the increase in resistance, or the blocked nozzle.

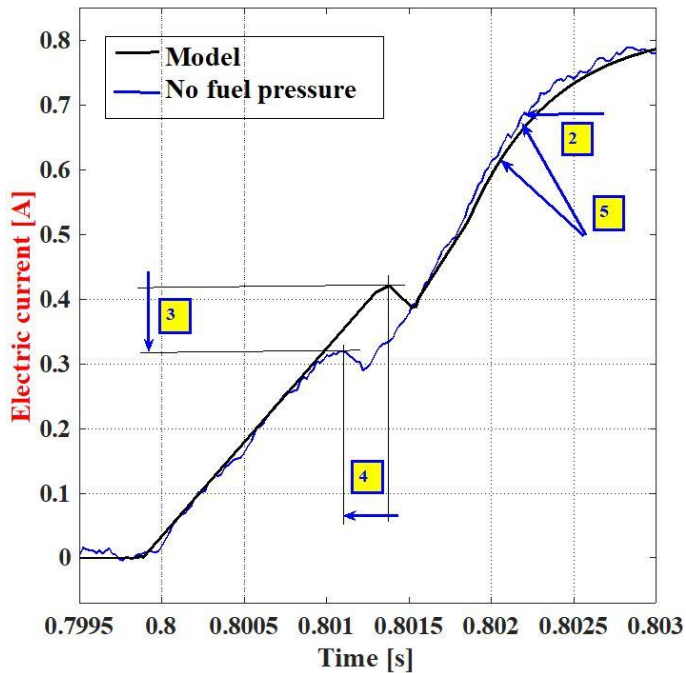


Fig. 9. Residuals #2 to #5 – in the case of lack of injection pressure.

The lack of injection pressure manifests as a significant decrease in the electric current at the point of the needle lifting marked as residual #3 (Fig. 9) and a negative phase shift denoted as residual #4. The lack of fuel pressure causes an earlier lifting of the needle. As a consequence of the lack of the most important force resulting from the fuel pressure, a smaller magnetic force (2) suffices to lift the needle. Therefore, a value sufficient to carry out this action will have been reached earlier. It is quite evident, that due to the lack of the injection pressure, the fuel flow does not take place.

#### 4.5 Blockage of injector needle and damage of return spring

When the injector needle is blocked, the electric current increases exponentially to the steady state – red line in Fig. 10. There is no characteristic bend in the current waveform, related to the needle lifting (residual #3). Due to the lack of movement of the needle, there is no change in the injector core inductance, or magnetic resistance. The magnetic force and the needle do not

perform any work, so the electric current increases steadily but is shifted in phase (residual #2). Because of the continuous increase in the electric current, there is a change in the angle of the curve representing the current increase (residual #5). The lack of the second transient state is quite obvious (waveform of the decaying voltage) – residual #7, determining the needle lowering onto the outlet socket. Such a characteristic, in the situation of a steady increase of the electric current increase, is described by the Kirchhoff's Equation (9) without the coefficients from Equation (1).

$$I(t) = \frac{\varepsilon_0}{R} \left( 1 - \exp\left(-\frac{R}{L}t\right) \right) \quad (9)$$

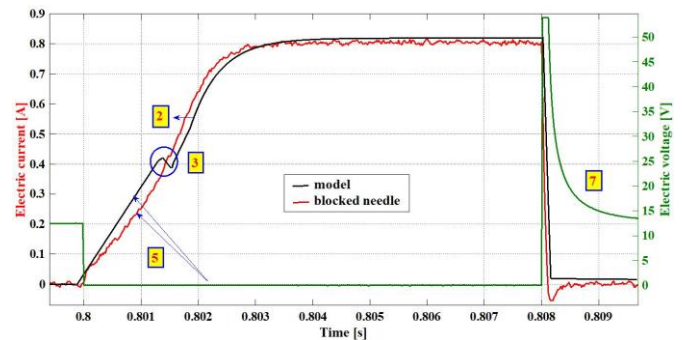


Fig. 10. Residuals #2, #3, #5, and #7 occurring with the blocked injector needle.

The damaging of the injector return spring results in a change of the point of the needle lowering, which will ensue the shift of the point, where the derivative  $\frac{dU_L}{dt} = 0$  (100-microsecond flattening of the curve of voltage decay, e.g. Fig. 5), which determines the needle stoppage in the nozzle. The shift of the point  $\frac{dI}{dt} = 0$  may occur, determining the needle lifting in the phase, and the values of the electric current. As a result of the return spring damage, the injector will not be able to efficiently cut the fuel flow off. Such a change can be detected using the traditional diagnostic methods.

Table 1 shows collectively all changes corresponding to the specific faults. In the successive columns, there is a trend in changes depicted as well as their type. It can be observed that a specific set of residuals matches a given damage. After a set of residuals has been identified, the type of damage can be determined.

Table 1. Overview of faults and corresponding changes in electric current-related waveforms.

Residuals	Type of fault					
	Short circuit	Resistance increase	Nozzle blocked	No fuel pressure	Blocking the needle	Damage of the return spring
1	↑	↓	0	0	0	0
2	↑	↓	↓	↑	↓	0
3	↑	↓	↑	↓	No change in sign of the waveform derivative	↓
4	–	+	+	–		–
5	+	↓	↑	↑	↓	0
6	↓	0	0	0	No change in sign of the waveform derivative	0
7	↑	0	0	0		↓
8	+	0	0	0		+

The successive columns differ significantly from each other, so damage can be easily identified.

## 5. Conclusions

The residual quantities include: values of electric current and voltage at specific points of characteristics (determining phases in the valve operation), maximal value of the electric current – the steady state shifts of these points in time, and inclination of the electric current waveform relative to the horizontal axis, the axis of time. They are a measure of the deviation from the expected electric signal waveforms. Their occurrence indicates the presence of damage in the injection system. Such an evaluation of the injector technical state can be performed in the real time, during its work, using a modified controller managing the dosing process. The residual quantities relative to the electric current or voltage values at characteristic points of the waveform depend on the pressure before the injector, thus, their use as a diagnostic parameter makes sense in relation to the same values of the injection pressure that could be obtained from the fuel pressure sensor.

## Acknowledgements

Project financed by the National Centre for Research and Development as part of the program for defense and security of the state.

## References

1. Allocca L, Siano D, Montanaro A, Panza MA. Imaging and Vibro-Acoustic Diagnostic Techniques Comparison for a GDI Fuel Injector. SAE International, Warrendale PA 2019, <https://doi.org/10.4271/2019-24-0058>.
2. Bogusz W, Grabarczyk J, Krok Franciszek. Podstawy Fizyki. Oficyna Wydawnicza Politechniki Warszawskiej 2016. ISBN: 978-83-7814-511-0.
3. Bor M, Borowczyk T, Karpiuk W, Smolec R. Determination of the response time of new generation electromagnetic injectors as a function of fuel pressure using the internal photoelectric effect. International Interdisciplinary PhD Workshop 2018; 335-339, <https://doi.org/10.1109/IIPHDW.2018.8388385>.
4. Bozhkov S, Milenov I, Slivarov O, Staneva G, Bozhkov P. Researching the waveforms of the automobile electromagnetic actuators. Facta Universitatis, Series: Automatic Control and Robotics 1 2016 (1–7).
5. Cammalleri M, Pipitone E, Beccari S, Genchi GA. Mathematical model for the prediction of the injected mass diagram of a S.I. engine gas injector. Journal of Mechanical Science and Technology 2013 (27), <https://doi.org/DO10.1007/s12206-013-0848-6>.
6. Dziubiński M, Adamiec M, Siemionem E, Drozd A. Experimental tests of the ignition-injection system. IOP Conference Series Materials Science and Engineering 2018; 421(2):022005, <https://doi.org/10.1088/1757-899X/421/2/022005>.
7. Ferdowski H, Cai J, Jagannathan S. Actuator and Sensor Fault Detection and Failure Prediction for Systems with Multi-dimensional Nonlinear Partial Differential Equations. International Journal of Control Automation and Systems 2022; 20(3):789-802, <https://doi.org/10.1007/s12555-019-0622-3>.
8. Figlus T, Konieczny Ł, Burdzik R, Czech P. The effect of damage to the fuel injector on changes of the vibroactivity of the diesel engine during its starting. JVE International LTD. Vibroengineering Procedia 2015; 6: 180-184.
9. Gawlica T, Samenfink W, Schünemann E, Koch T. Model-based optimization of multi-hole injector spray targeting for gasoline direct injection. Tagung Einspritzung und Kraftstoffe, Springer Fachmedien 2019; 271–289, [https://doi.org/10.1007/978-3-658-23181-1\\_14](https://doi.org/10.1007/978-3-658-23181-1_14).
10. Gritsenko A, Shepelev V, Zadorozhnaya E, Shubenkova K. Test diagnostics of engine systems in passenger cars FME Transactions 2020; 48: 46–52, <https://doi.org/10.5937/fmet2001046G>.
11. Hung NB, Lim OT. A simulation and experimental study on the operating characteristics of a solenoid gas injector. Advances in Mechanical Engineering 2019;11, <https://doi.org/10.1177/1687814018817421>.
12. Isermann R. Model-Based Fault Detection and Diagnosis - Status and Applications. IFAC Proceedings Volumes, 2004; 37. <https://doi.org/10.1016/j.arcontrol.2004.12.002>.
13. Isermann R. Mechatronic systems: fundamentals. Springer, London 2005. ISBN: 978-1-84628-259-1.
14. Isermann R. Advanced model-based diagnosis of internal combustion engines. Internationaler Motorenkongress Springer Fachmedien 2016; 413–432, [https://doi.org/10.1007/978-3-658-12918-7\\_27](https://doi.org/10.1007/978-3-658-12918-7_27).

15. Ismail MAA, Wiedemann S, Bosch C, Stuckmann C. Design and Evaluation of Fault-Tolerant Electro-Mechanical Actuators for Flight Controls of Unmanned Aerial Vehicles Actuators 2021; 10: 175, <https://doi.org/10.3390/act10080175>.
16. Jianmin L, Yupeng S, Xiaoming Z, Shiyong X, Lijun D. Fuel Injection System Fault Diagnosis Based on Cylinder Head Vibration Signal. *Procedia Engineering*, 2011; 16, <https://doi.org/10.1016/j.proeng.2011.08.1075>.
17. Khameneian A, Wang X, Dice P, Naber JD, Shahbakhti M, Archer C, Moilanen P, Glugla C, Huberts GA. Real-time control-oriented discrete nonlinear model development for in-cylinder air charge, residual gas and temperature prediction of a Gasoline Direct Injection engine using cylinder, intake and exhaust pressures. *Control Engineering Practice* 2022; 119, <https://doi.org/10.1016/j.conengprac.2021.104978>.
18. Komorska I, Wołczyński Z, Borczuk A. Model-based analysis of sensor faults in SI engine. *Combustion Engines* 2017, <https://doi.org/10.19206/CE-140240>.
19. Leach F, Davy MH, Henry MP, Tombs M, Zhou F. A New Method for Measuring Fuel Flow in an Individual Injection in Real Time. *SAE International Journal of Engines* 2018; 11: 687–696, <https://doi.org/10.4271/2018-01-0285>.
20. Li S, Nehl T, Gopalakrishnan S, Omekanda A, Namuduri C, Prasad RA. Dynamic Solenoid Model for Fuel Injectors. *IEEE Energy Conversion Congress and Exposition* 2018; 3206–3213, <https://doi.org/10.1109/ECCE.2018.8558394>.
21. Lin TR, Tan ACC, Mathew J. Condition monitoring and diagnosis of injector faults in a diesel engine using in-cylinder pressure and acoustic emission techniques. *Dynamics for Sustainable Engineering*, The HongKong Polytechnic University 2011.
22. Mazzoleni M, Di Rito G, Previdi F. Fault Diagnosis and Condition Monitoring Approaches. *Electro-Mechanical Actuators for the More Electric Aircraft*, Springer International Publishing 2021; 87–117, [https://doi.org/10.1007/978-3-030-61799-8\\_3](https://doi.org/10.1007/978-3-030-61799-8_3).
23. Mączak J, Jasiński M. Model-based detection of local defects in gears. *Arch Appl Mech* 2018; 8, <https://doi.org/10.1007/s00419-017-1321-2>.
24. Merola SS, Tornatore C, Sementa P. Optical investigation of the fuel injector influence in a PFI spark ignition engine for two-wheel vehicles. *Journal of Mechanical Science and Technology* 2012; 26, <https://doi.org/10.1007/s12206-011-0801-5>.
25. Moshou D, Natsis A, Kateris D, Pantazi XE, Kalimanis I, Gravalos I. Fault Detection of Fuel Injectors Based on One-Class Classifiers. *Modern Mechanical Engineering* 2013; 4, <https://doi.org/10.4236/mme.2014.41003>.
26. Nogin S, Semião J, Monteiro JA. Non-intrusive IoT System for the Detection of Faults in Internal Combustion Engines. *Springer International Publishing* 2018; 338–358, [https://doi.org/10.1007/978-3-319-70272-8\\_28](https://doi.org/10.1007/978-3-319-70272-8_28).
27. Papadopoulos PM, Lympelopoulou G, Polycarpou MM, Ioannou P. Distributed Diagnosis of Sensor and Actuator Faults in Air Handling Units in Multi-Zone Buildings: A Model-Based Approach. *Energy and Buildings* 2022; 256, <https://doi.org/10.1016/j.enbuild.2021.111709>.
28. Pielech A, Skowron M, Mazanek A. Evaluation of the injectors operational wear process based on optical fuel spray analysis. *eksploatacja i niezawodność – Maintenance and reliability* 2018; 20 (1): 83–89, <https://doi.org/10.17531/ein.2018.1.11>.
29. Putwattana S, Nivesrangsan P. The study of fuel injector operation using acoustic emission signals. *5th International Conference on Business and Industrial Research* 2018, <https://doi.org/10.1109/ICBIR.2018.8391208>.
30. Radkowski S. Use of vibroacoustical signal in detecting early stages of failures. *Eksploatacja i Niezawodność – Maintenance and Reliability* 2007; 3: 11-18, <https://doi.org/10.17531/ein>.
31. Rochussen J, Son J, Yeo J, Khosravi M, Kirchen P, McTaggart-Cowan G. Development of a Research-Oriented Cylinder Head with Modular Injector Mounting and Access for Multiple In-Cylinder Diagnostics. *SAE International* 2017, <https://doi.org/10.4271/2017-24-0044>.
32. Sarwar A, Sankavaram C, Lu X. Diagnosis and Prognosis of Fuel Injectors based on Control Adaptation. *Prognostics and Health Management Society* 2017.
33. Sebok M, Jurcik J, Gutten M, Kornciak D, Roj J, Zukowski P. Diagnostics and measurement of the gasoline engines injection system. *Przegląd Elektrotechniczny* 2015; 1, <https://doi.org/10.15199/48.2015.08.20>.
34. Sebok M, Gutten M, Adamec J, Glowacz A, Roj J. Analysis of The Electronic Fuel Injector Operation. *Communications - Scientific Letters of the University of Zilina* 2018; 20: 32–36, <https://doi.org/10.26552/com.C.2018.1.32-36>.
35. Taha Z, Rahim MA, Mamat R. Injection characteristics study of high-pressure direct injector for Compressed Natural Gas using experimental and analytical method. *IOP Conference Series Materials Science and Engineering* 2017; 257 (1): 012057, <https://doi.org/10.1088/1757-899X/257/1/012057>.
36. Tan T, Park JS, Leteinturier P. Enhanced Injector Dead Time Compensation by Current Feedback. *SAE International* 2016, <https://doi.org/10.4271/2016-01-0088>.
37. Wang L, Huang H, Lin Z, Meng F. Advanced gasoline engine misfire diagnostic method based on crankshaft speed multiple filtering. *International Conference on Electric Information and Control Engineering* 2011, <https://doi.org/10.1109/ICEICE.2011.5776855>.
38. Wang P, Yu C. Distributed Actuator Fault Detection of LDTV Systems Using Relative Output Measurements. *40th Chinese Control Conference* 2021; 4449–4454, <https://doi.org/10.23919/CCC52363.2021.9550647>.
39. Więclawski K, Mączak J, Szczerowski K. Electric current as a source of information about control parameters of indirect injection fuel injector. *Eksploatacja i Niezawodność – Maintenance and Reliability* 2020; 22: 449–454, <https://doi.org/10.17531/ein.2020.3.7>.

40. Więclawski K, Mączak J, Szczurowski K. Electric Current Waveform of the Injector as a Source of Diagnostic Information. *Sensors* 2020; 20, <https://doi.org/10.3390/s20154151>.
41. Więclawski K, Walczak D, Mączak J, Radkowski S, Szczurowski K, Zieliński Ł. Method of controlling a fuel injector controller and a fuel injector controller. 2020; Patent, Espacenet: PL235122B1.
42. Wu S, Xu M, Hung DLS, Li T, Pan H. Near-nozzle spray and spray collapse characteristics of spark-ignition direct-injection fuel injectors under sub-cooled and superheated conditions. *Fuel* 2016; 183: 322–334, <https://doi.org/10.1016/j.fuel.2016.06.080>.
43. Yasukawa Y, Ishii E, Yoshimura K, Ogura K. Fuel Spray Analysis Near Nozzle Outlet of Fuel Injector During Valve Movement. *Tagung Diesel- Und Benzindirekteinspritzung, Springer Fachmedien*. 2017; 345–362, [https://doi.org/10.1007/978-3-658-15327-4\\_17](https://doi.org/10.1007/978-3-658-15327-4_17).